Inhibition of Cancer Cell Growth by Ruthenium(II) Arene Complexes

Robert E. Morris,[†] Rhona E. Aird,[‡] Piedad del Socorro Murdoch,[†] Haimei Chen,[†] Jeff Cummings,[‡] Nathan D. Hughes,[†] Simon Parsons,[†] Andrew Parkin,[†] Gary Boyd,[‡] Duncan I. Jodrell,[‡] and Peter J. Sadler*[,†]

Department of Chemistry, University of Edinburgh, West Mains Road, Edinburgh EH9 3JJ, U.K., and Imperial Cancer Research Fund, Medical Oncology Unit, Western General Hospital, Edinburgh EH4 2XU, U.K.

Received January 31, 2001

Inhibition of the growth of the human ovarian cancer cell line A2780 by organometallic ruthenium(II) complexes of the type [(η^6-arene)Ru(X)(Y)(Z)], where arene is benzene or substituted benzene, X, Y, and Z are halide, acetonitrile, or isonicotinamide, or X,Y is ethylenediamine (en) or *N*-ethylethylenediamine, has been investigated. The X-ray crystal structures of the complexes [(η^6-*p*-cymene)Ru(en)Cl]PF_6 (**5**), [(η^6-*p*-cymene)$RuCl_2$(isonicotinamide)] (**7**), and [(η^6-biphenyl)Ru(en)Cl]PF_6 (**9**) are reported. They have "piano stool" geometries with η^6 coordination of the arene ligand. Complexes with X,Y as a chelated en ligand and Z as a monofunctional leaving group had the highest activity. Complexes **5**, **6** (the iodo analogue of **5**), **9**, and **10** (ethylethylenediamine analogue of **9**) were as active as carboplatin. Hydrolysis of the reactive Ru−Cl bond in complex **5** was detected by HPLC but was suppressed by the addition of chloride ions. Complex **5** binds strongly and selectively to G bases on DNA oligonucleotides to form monofunctional adducts. No inhibition of topoisomerase I or II by complexes **5**, **6**, or **9** was detected. These chelated Ru(II) arene complexes have potential as novel metal-based anticancer agents with a mechanism of action different from that of the Ru(III) complex currently on clinical trial.

Introduction

The success of cisplatin and related platinum complexes as anticancer agents has stimulated a search for other active transition metal anticancer complexes, and ruthenium in particular has attracted recent attention.[1] The activity of *fac*-[$Ru^{III}Cl_3(NH_3)_3$] was discovered early,[2] but its poor aqueous solubility prevented further use. Since then, complexes such as *trans*-[HIn][$Ru^{III}Cl_4$-$(Ind)_2$] (Ind = indazole), *mer*-[Ru^{III}(terpy)Cl_3] (terpy = 2,2′-terpyridine), and [Ru^{IV}(chd-H_2)Cl_2] (chd = 1,2-cyclohexanediaminetetraacetate) have also been reported to be highly active.[3−5] The complex *trans*-[HIm]-[$Ru^{III}Cl_4$(DMSO)(Im)] (NAMI-A) has a low cytotoxicity but is active against tumor metastases and has recently entered clinical trials.[6]

Some Ru(III) complexes are known to bind to Fe(III) sites of the proteins lactoferrin and transferrin,[7,8] and transferrin is thought to be responsible for the delivery of Ru(III) to cancer cells where it is taken up via receptor-mediated endocytosis.[9] Transferrin normally transports Fe(III) in the blood but is only about one-third occupied by Fe(III), and so there are vacant sites available for Ru(III) binding. Another important step in the mechanism of action of Ru(III) complexes is thought to be in vivo reduction to Ru(II), which is kinetically more reactive than Ru(III). In view of this we have investigated the design of cytotoxic organometallic Ru(II) arene complexes. Arene ligands stabilize Ru(II) and also provide a hydrophobic face for the complex, which might enhance biomolecular recognition processes and transport of ruthenium through cell membranes. The organometallic Ti^{IV} complex titanocene dichloride is currently on clinical trials as an anticancer drug.[1] We report here that monofunctional Ru(II) complexes of the type [(η^6-arene)Ru^{II}(en)X]$^+$ (X = halide) are effective inhibitors of the growth of cancer cells and form strong monofunctional adducts with DNA.

Results and Discussion

Synthesis and Characterization. We have synthesized ruthenium(II) complexes of the type [(η^6-arene)-Ru(X)(Y)(Z)] in which the π-bonded arene is benzene or a substituted benzene, X, Y, and Z are monodentate ligands such as halide, acetonitrile, and nicotinamide, or X,Y is the chelating ligand ethylenediamine or *N*-ethylethylenediamine. The presence of the arene leads to the stabilization of Ru(II), and the complexes do not readily undergo oxidation to Ru(III). Moreover, most of the compounds are ionic and have a reasonable aqueous solubility.

We determined the X-ray crystal structures of [(η^6-*p*-cymene)Ru(en)Cl]PF_6 (**5**, Figure S1 of Supporting Information), [(η^6-*p*-cymene)$RuCl_2$(isonicotinamide)] (**7**, Figure S2 of Supporting Information), and [(η^6-biphenyl)Ru(en)Cl]PF_6 (**9**, Figure 1). All have the characteristic "piano-stool" geometry of Ru(II) arene complexes, with an η^6 π-bonded arene ring forming the seat and three other ligands forming the legs of the stool. The structures of the other complexes are similar. The Ru−N bond lengths in complexes **5**, **7**, and **9** are within the range 2.11−2.14 Å, Ru−Cl is 2.39−2.45 Å, and N−Ru−N angles are 78.2−79.2°, values close to those reported previously for related Ru^{II} arene complexes.[10,11] The X-ray structure of complex **9** [(η^6-biphenyl)Ru(en)Cl]PF_6 (Figure 1) is the first of a monoarene complex of ruthenium where the arene is biphenyl. The only other

* To whom correspondence should be addressed. Phone: +44-131-650-4729. Fax: +44-131-650-6452. E-mail: P.J.Sadler@ed.ac.uk.
[†] University of Edinburgh.
[‡] Western General Hospital.

10.1021/jm010051m CCC: $20.00
Published on Web 10/03/2001

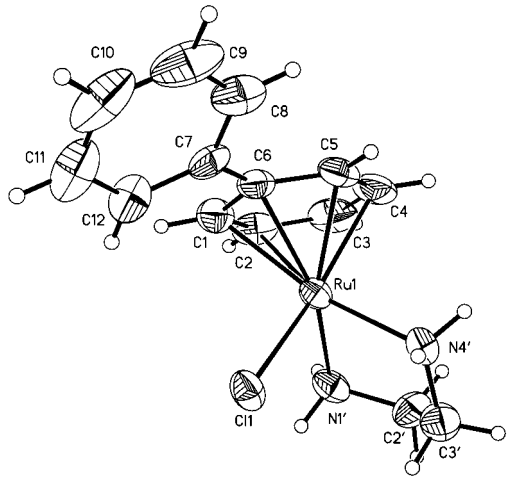

Figure 1. X-ray crystal structure of the cation in complex **9** [(η^6-biphenyl)Ru(en)Cl][PF_6] (thermal ellipsoids at 50% level). The longest Ru−C bond to the substituted C (2.244(6) Å) is 0.054 Å longer than the other Ru−C bonds; Ru−N1′ 2.110(5) Å, Ru−N4′ 2.121(5) Å, Ru−Cl 2.4080(15) Å. The phenyl rings of the biphenyl ligand are tilted from coplanarity by 24.6°. The PF_6^- anion (not shown) is disordered.

Ru(η^6-biphenyl) complex previously reported is the bis-arene complex [bis(η^6-biphenyl)Ru^{II}][BF_4]$_2$, the biphenyl analogue of ruthenocene. Both the preliminary structure of [bis(η^6-biphenyl)Ru^{II}][BF_4]$_2$ reported in 1990[12] and the more detailed structure reported in 1995 [13] show that the two phenyl rings of the biphenyl ligand are twisted from coplanarity by ca. 25.0°. This phenomenon is also seen in complex **9**, for which one phenyl ring is twisted out of the plane by 24.6° (Figure 1). In the X-ray structure of the ligand itself, free biphenyl is planar.[14] The twisting probably results from packing effects in the crystal. It is notable that the length of the bond between Ru and the substituted carbon, 2.244(6) Å, is 0.054 Å longer than any of the other Ru−C bonds in the molecule. This has also been reported[13] to be the case for [Ru^{II}(η^6-biphenyl)$_2$][BF_4]$_2$ for which the Ru−C(substituted) bond lengths of 2.271(5) and 2.262(7) Å are also longer than the other Ru−C bonds. The isonicotinamide ligand in complex **7** is coordinated through the pyridyl nitrogen, and there is intermolecular hydrogen bonding between the N−H of the amide on one molecule and the amide oxygen of an adjacent molecule (NH···O, 1.984 Å).

It has been reported previously that (η^6-C_6H_6)Ru(II) bonds resist hydrolysis and are relatively stable in water.[15] The arene ligand not only provides a lipophilic side to the complex but also stabilizes Ru in the +2 oxidation state. Oxidation of (η^6-C_6H_6)Ru(II) complexes to Ru^{III} is unfavorable. Complex **5** exhibited good solubility in water and appeared to undergo rapid aquation (substitution of bound Cl by H_2O). Three HPLC peaks were detected from a 10 mM aqueous solution of **5** within minutes of dissolution using a reverse-phase column and elution with ammonium acetate and 1-pentanesulfonate as ion-pairing agent (Figure S3 of Supporting Information). The HPLC peaks were identified by positive-ion LC−ESI-MS (Figure S4 of Supporting Information). Peaks a and b with retention times of 8.4 and 10 min can be assigned to adducts with water and with the ion-pairing agent, respectively, and gave rise to ESI-MS peaks at *m*/*z* 315 and *m*/*z* 447 corresponding to the aqua adduct (calcd, 314) and to an adduct with the ion-pairing agent (calcd, 447). The peak with a retention time of 10.8 min (peak c) gave an ESI-MS peak at *m*/*z* 331, consistent with the initial complex [(η^6-*p*-cymene)Ru(en)Cl]$^+$ (calcd, 331). The fragment {(η^6-*p*-cymene)Ru(en)−H}$^+$ was also detected (*m*/*z* 295). The ratio of a:b:c was 28:12:60 but changed to 59:29:12 for a more dilute solution of complex **5** (0.2 mM). When complex **5** was dissolved in 100 mM NaCl (i.e., a concentration close to physiological), hydrolysis was largely suppressed, with 81% of **5** remaining intact in a 10 mM solution and with >99% remaining intact for a 0.2 mM solution of **5**.

Table 1. Inhibition of Growth of A2780 Human Ovarian Cancer Cells after Exposure to Ru(II) Compounds for 24 h

complex[a]	IC_{50} [b] (μM)
[(η^6-*p*-cymene)RuCl(CH_3CN)$_2$]PF_6, **1**	>150
[(η^6-*p*-cymene)RuBr(CH_3CN)$_2$]PF_6, **2**	>150
[(η^6-C_6H_6)RuCl(en)]PF_6, **3**	17
[(η^6-C_6H_6)RuI(en)]PF_6, **4**	20
[(η^6-*p*-cymene)RuCl(en)]PF_6, **5**	9
[(η^6-*p*-cymene)RuI(en)]PF_6, **6**	8
[(η^6-*p*-cymene)RuCl$_2$(isonicotinamide)], **7**	>150
[(η^6-$C_6H_5CO_2CH_3$)RuCl(en)]PF_6, **8**	55
[(η^6-$C_6H_5C_6H_5$)RuCl(en)]PF_6, **9**	6
[(η^6-$C_6H_5C_6H_5$)RuCl(en-Et)]PF_6, **10**	6
carboplatin	6
cisplatin	0.5

[a] en = ethylenediamine; en-Et = *N*-ethylethylenediamine. [b] All compounds were evaluated at least five times with the exception of compounds **8**, **10**, and carboplatin. Standard deviations were normally within the range 10−51%.

Cancer Cell Growth Inhibition. A2780 cells were plated on day zero, and Ru(II) arene complexes were added on day 3. The complex was removed on day 4 (i.e., 24 h cell exposure), and after growth in fresh medium in the absence of drug, the cells were counted on day 7. Because it is known that metal coordination complexes can undergo ligand substitution reactions with components of the media in which they are dissolved, freshly made stock solutions of each compound were used. The complexes were stored in the dark at 277 K as a precaution against photochemical decomposition. The IC_{50} values are listed in Table 1. It was possible to obtain reproducible IC_{50} values for most of the complexes, but notable exceptions were those containing three reactive coordination sites (complexes **1**, **2**, and **7**) for which there was a marked decrease in potency when tested over a period of 12 weeks. Complexes **5**, **6**, **9**, and **10** caused growth inhibition of the human ovarian cancer cell line A2780 with IC_{50} values of 6−9 μM. Although this is an order of magnitude less than cisplatin (IC_{50} of 0.5 μM), the potency is similar to that of the anticancer drug carboplatin.

Binding to Oligonucleotides. Next we investigated reactions of complex **5** with the DNA 14-mer d($A_1T_2A_3$-$C_4A_5T_6G_7G_8T_9A_{10}C_{11}A_{12}T_{13}A_{14}$) **I** in aqueous solution in 1:1, 2:1, and 5:1 mole ratios, pH 6.42, 310 K, using HPLC (reverse-phase C8, 300 Å) to separate the products. For the 1:1 (100 μM) reaction after 24 h, new peaks d (5.7 min), e (7.9 min), and f (13.4 min) were detected, as well as a peak for unreacted **I** (3.8 min) (Figure 2), on elution with 20 mM triethylammonium acetate and an acetonitrile gradient. These peaks were identified by negative ion mode ESI-MS as two monoruthenated adducts (peaks d and e *m*/*z* 4566.0, calcd 4564.9; Figure

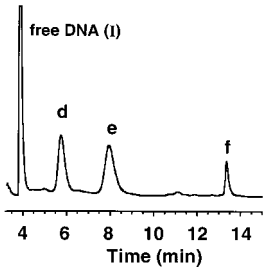

Figure 2. Separation of the products from reaction of complex **5** with the DNA 14-mer **I** (1:1 mole ratio, 100 μM, 310 K, 24 h) by HPLC on a reverse-phase C8 column with 20 mM triethylammonium acetate and an acetonitrile gradient. Peaks d and e are due to monoruthenated adducts, and peak f is due to a diruthenated adduct.

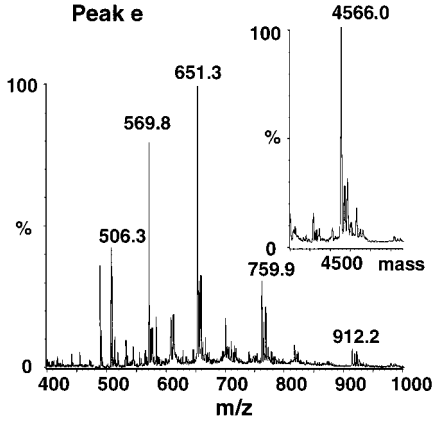

Figure 3. Negative ion ESI-MS of peak e from the HPLC separation of the products of the reaction of complex **5** with the DNA 14-mer **I** (Figure 2). The multiply charged ion series originates from the monoruthenated adduct **I**-{(η^6-*p*-cymene)-Ru(en)}. The spectrum of HPLC peak d was almost identical, and therefore, these peaks correspond to isomers with different ruthenation sites: (peak d) 3′G-Ru; (peak e) 5′G-Ru (see Figure 2).

3) and a bisruthenated adduct, peak f (*m/z* 4859.4, calcd 4861.0). The ratio of d:e:f was 3.6:4.8:1. To identify the sites of ruthenation (by {η^6-*p*-cymene)Ru(en)}$^{2+}$), the adducts were digested with snake venom phosphodiesterase (VPD), a 5′-exonuclease that begins digestion at the 3′-end of DNA. Sequence ladders were constructed by combining transformed mass spectra after various digestion times. These showed that for peak d Ru is bound to the 3′-G (G8) of **I**, for peak e oligonucleotide **I** is ruthenated at the 5′-G (G7, Figure S5 of Supporting Information), and for peak f, **I** is ruthenated on both Gs. The time dependence of the 1:1 reaction was studied by HPLC and showed that the reaction was complete within 4 h at 310 K. At higher Ru/I mole ratios, the proportion of peak f increased relative to peaks d and e, so at a 5:1 mole ratio bisruthenated **I** was the only species detected. The formation of some bisruthenated **I** even after addition of only 1 mol equiv of complex **5** was notable. The downfield shift of the ^{1}H NMR H8 resonance of 5′ GMP from 8.2 to 8.9 ppm on reaction of complex **5** in a 1:1 mole ratio, pH 7.43, suggested that binding of Ru^{II} to G occurs via N7. This was confirmed by a ^{1}H NMR pH titration: no shift of H8 was observed over the normal pH range for N7 protonation (1.9−4.0). Although N7 of G, the most electron-dense site on DNA, is known to be a target for both Ru^{II} and Ru^{III},[16−18] many previously reported Ru

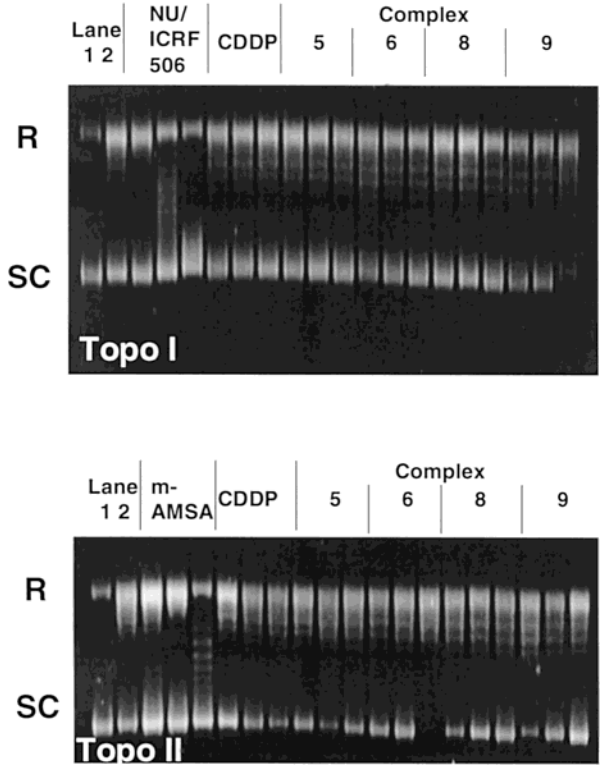

Figure 4. Topoisomerase relaxation assays showing agarose gels stained with ethidium bromide. Enzyme activity is characterized by conversion of pBR322 plasmid DNA from the supercoiled conformation (SC, form I) to the fully relaxed conformation (R, form II; see lanes 1 and 2). DNA species migrating between these two bands represent either partially relaxed or over-relaxed conformations. Drug concentrations are 1, 10, and 50 μM. Lane 1 contains pBR322 DNA substrate, and lane 2 contains DNA + topo enzyme. The top part of the figure shows topoisomerase I assays. NU/ICRF 506 (lanes 3−5) reduced the intensity of form II in a dose-dependent manner, with 10 μM producing 50% enzyme inhibition, whereas none of the Ru(II) complexes tested (**5**, **6**, **8**, and **9**) inhibited Topo I catalytic activity over the concentration range 1−50 μM. In the bottom part of the figure, topoisomerase II assays show a similar pattern, for which m-AMSA was included as the positive control (lanes 3−5).

complexes are not as base-selective as complex **5** and act as intra- or interstrand cross-linking agents because they have more than one reactive coordination site,[1] whereas complex **5** is a monofunctional agent. The complex [Ru(η^6-C_6H_6)$(D_2O)_3$]$^{2+}$, for example, has three coordination sites that readily react with nucleotides.[16]

DNA melting experiments were carried out on duplex **III**, formed from the 14-mer strand **I** and its complementary strand **II**, to investigate whether adducts with complex **5** destabilized the duplex structure. Melting curves were determined for a solution of **III** (in 10 mM phosphate buffer, 50 mM $NaClO_4$) and complex **5** or cisplatin in a 1:1 mole ratio (3 μM) for 4 days at ambient temperature. The T_M for **III** of 313.1 K was lowered to 310.2 K by cisplatin and also by complex **5**. Cisplatin is expected to form intrastrand GG cross-links under these conditions. Monofunctional adducts of **5** with the G bases may also distort duplex DNA. Recently it has been suggested that active trans Pt(II) imino ether anticancer complexes that form monofunctional adducts can induce 50° bends in DNA.[19]

Inhibition of Topoisomerase. Figure 4 shows an agarose gel stained with ethidium bromide illustrating

a typical Topo I relaxation assay. Enzyme activity is characterized by conversion of the DNA substrate from the supercoiled conformation (form I) to the fully relaxed conformation (form II; see lanes 1 and 2 of Figure 4). DNA species migrating between these two bands are referred to as topomers and represent either partially relaxed or, more commonly, over-relaxed conformations.[20,21] NU/ICRF 506 reduced the intensity of form II in a dose-dependent manner, with 10 μM producing 50% enzyme inhibition, in keeping with previous reports.[22] None of the Ru(II) complexes tested (**5**, **6**, **8**, and **9**) inhibited Topo I catalytic activity over the concentration range 1−50 μM. A similar pattern was observed with Topo II catalyzed DNA relaxation, where m-AMSA was included as the positive control (lanes 3−5 of Figure 4). Under the conditions used here, cisplatin was also without effect in both Topo I and II relaxation assays.

Because complexes **5**, **6**, and **9** all inhibited the growth of human ovarian cancer cells with IC_{50} values of less than 10 μM (see Table 1) and had no effect on the activity of either Topo I or Topo II up to 50 μM, it is unlikely that inhibition of these enzymes is responsible for their anticancer activity. Recently, the bifunctional organo-Ru(II) complex $[RuCl_2(C_6H_6)(dmso)]$ (RuBen) has been shown to inhibit the catalytic activity of Topo II and to stabilize the cleavable complex.[23] This mechanism was claimed to be critical for antiproliferative activity. However, RuBen is almost 2 orders of magnitude less potent as a cell growth inhibitor than complexes in the present series of Ru(II) complexes. In aqueous solution, RuBen is probably hydrolyzed[1] to *fac*-$[Ru(\eta^6\text{-}C_6H_6)(H_2O)_3]^{2+}$, and such a trifunctional ion could clearly react differently from the monofunctional species used in our work.

Conclusion

The water-soluble chelated organometallic Ru(II) complexes $[(\eta^6\text{-}p\text{-cymene})Ru(en)(X)]^+$, where X = Cl (**5**) or I (**9**), and $[(\eta^6\text{-}C_6H_5C_6H_5)RuCl(YZ)]^+$, where Y, Z = ethylenediamine or *N*-ethylethylenediamine, inhibit the growth of A2780 human ovarian cancer cells with a potency similar to that of the anticancer drug carboplatin. X-ray crystal structures show that these Ru(II) arene complexes have piano stool structures, and HPLC−MS studies showed that complex **5** undergoes aquation in aqueous solution, which can be suppressed by addition of NaCl. Since extracellular chloride concentrations tend to be higher than intracellular chloride levels, aquation may activate chloro-Ru(II) arene complexes inside cells prior to reactions with DNA, as is the case for cisplatin. The complexes are not inhibitors of topoisomerase but bind strongly and selectively to guanine bases on DNA, forming monofunctional adducts. When the design of this class of complexes is optimized, it may be possible to target specific DNA base sequences. The mechanism of action of these Ru(II) organometallic complexes is likely to be different from that of the existing Ru(III) drug NAMI-A.

Experimental Section

Materials. The starting materials $[(\eta^6\text{-arene})RuX_2]_2$ (X = halide) were prepared according to a previously reported precedure.[24,25] Acetonitrile was dried over CaH_2, alcohols were dried and distilled from P_2O_5, and ethylenediamine was distilled over Na metal prior to use. The HPLC-purified sodium salts of 14-mer oligonucleotides **I** and **II** were obtained from Oswel (Southampton, U.K.). Snake venom phosphodiesterase (VPD) was purchased from Sigma Chemical Co. (Poole, U.K.), human topoisomerase I and II from TopoGEN Inc. (Ohio), and pBR322 supercoiled plasmid DNA from Boehringer Mannheim (Mannheim, Germany). All other reagents were obtained from commercial suppliers and used as received.

Instrumental Methods. ^{1}H NMR spectra were recorded on Bruker DMX and Varian Inova spectrometers at 500 and 600 MHz, respectively, using sodium 3-trimethylsilylpropionic acid (TSP, $\delta = 0$) or dioxan ($\delta = 3.767$ ppm) as internal references. DNA melting curves were recorded on a Perkin-Elmer Lambda20 spectrometer using 1 cm path length quartz cells and a PTP1 Peltier temperature programmer. Negative and positive ion electrospray mass spectra were obtained on a Platform II mass spectrometer (Micromass, Manchester, U.K.). The samples were infused at a flow rate of 0.48 mL min^{-1}, and the ions were produced in an atmospheric pressure ionization (API)/ESI ion source. The temperature was 363 K, and the drying gas flow rate was 300 L h^{-1}. A cone voltage of 40 keV over 0−1500 Da was used. The acquisiton and deconvolution of data were performed on a Mass Lynx (version 2.3) Windows NT PC system using the Max Ent Electrospray software algorithm and calibrated vs a NaI calibration file. HPLC was carried out on a Hewlett-Packard series 1100 Chemstation. The chromatographic conditions were optimized on a Nucleosil C_8 300 Å stainless steel column (250 mm × 4.6 mm, 5 μm, Hichrom, U.K.), usually at 298 K. The detection wavelength was 254 nm, and the relative concentrations were determined from peak areas.

Syntheses. The preparations of compounds **1** and **2** were based on a published synthesis[26] and followed the same general procedure, as did the preparations of the ethylenediamine complexes **3**−**9** and *N*-ethylethylenediamine complex **10**.[27]

$[(\eta^6\text{-}p\text{-cymene})RuCl(CH_3CN)_2]PF_6$ (1). $[(\eta^6\text{-}p\text{-cymene})RuCl_2]_2$ (0.31 g, 0.51 mmol) was stirred in 20 mL of reagent grade acetonitrile, and NH_4PF_6 (0.18 g, 1.10 mmol) in 5 mL of acetonitrile was added in one portion. The flask was sealed without specific precautions to exclude air, and the reaction was stirred at ambient temperature. After 14 h the pale precipitate was filtered off and the orange filtrate evaporated to leave an orange solid. This was dissolved in a minimum of hot acetonitrile, filtered, and allowed to cool. Ether was added until precipitation was apparent, and the mixture was placed in a freezer at ca. 253 K for 2 days. The precipitate was filtered off, washed with ether, and dried in vacuo (0.28 g; 54.9% yield). ^{1}H NMR (CD_3CN): δ 5.35 (m, 2H), 5.28 (m, 2H), 1.23 (d, 6H). Anal. Calcd for $C_{14}H_{20}ClF_6N_2PRu$: C, 33.78; H, 4.05; N, 5.62. Found: C, 33.80; H, 3.91; N, 5.53.

$[(\eta^6\text{-}p\text{-cymene})RuBr(CH_3CN)_2]PF_6$ (2). 2 was prepared according to a published procedure[26] using $[(\eta^6\text{-}p\text{-cymene})RuBr_2]_2$ (0.24 g, 0.3 mmol), NH_4PF_6 (0.12 g, 0.74 mmol), and dry acetonitrile (12 mL). The final product was recrystallized from acetonitrile/ether to give deep-red crystals (0.28 g, 86.7% yield). ^{1}H NMR (CD_3CN): δ 5.44 (m, 2H), 5.36 (m, 2H), 1.26 (d, 6H). Anal. Calcd for $C_{14}H_{20}BrF_6N_2PRu$: C, 31.01; H, 3.72; N, 5.16. Found: C, 31.22; H, 3.75; N, 5.09.

$[(\eta^6\text{-}C_6H_6)RuCl(H_2NCH_2CH_2NH_2\text{-}N,N)]PF_6$ (3). $[(\eta^6\text{-}C_6H_6)RuCl_2]_2$ (0.167 g, 0.33 mmol) was suspended in dry methanol (50 mL), and ethylenediamine (0.06 g, 1 mmol) was added in one portion. The mixture was stirred for 3 h and filtered, and NH_4PF_6 (0.5 g, 3.07 mmol) was added. The volume was slowly reduced to ca. 15 mL on a rotary evaporator, and after standing at 277 K, the mixture formed a microcrystalline product. This was collected, washed with ether, and recrystallized from methanol/ether (0.128 g, 47.0% yield).^{1}H NMR (DMSO-d_6): δ 6.45 (b, 2H), 5.86 (s, 6H), 4.28 (b, 2H), 2.34 (m, 2H), 2.17 (m, 2H). Anal. Calcd for $C_8H_{14}ClF_6N_2PRu$: C, 22.89; H, 3.36; N, 6.67. Found: C, 22.81; H, 3.24; N, 6.51.

$[(\eta^6\text{-}C_6H_6)RuI(H_2NCH_2CH_2NH_2\text{-}N,N)]PF_6$ (4). The procedure followed that for compound **3**, using $[(\eta^6\text{-}C_6H_6)RuI_2]_2$ (0.48 g, 0.55 mmol), dry methanol (80 mL), ethylenediamine (0.12 g, 2 mmol), and NH_4PF_6 (0.5 g, 3.07 mmol) (0.412 g, 73.3% yield). ^{1}H NMR (DMSO-d_6): δ 6.42 (b, 2H), 5.86 (s, 6H),

4.22 (b, 2H), 2.35 (m, 2H), 2.15 (m, 2H). Anal. Calcd for $C_8H_{14}IF_6N_2PRu$: C, 18.80; H, 2.76; N, 5.48. Found: C, 18.52; H, 2.43; N, 5.14.

[(η^6-*p*-cymene)RuCl($H_2NCH_2CH_2NH_2$−*N,N*)]PF_6 (5). The procedure followed that for compound **3** using [(η^6-*p*-cymene)-$RuCl_2]_2$ (0.39 g, 0.64 mmol), methanol (60 mL), and ethylenediamine (0.12 g, 2.0 mmol). The reaction mixture was stirred for 1.5 h, and the green liquid was filtered. NH_4PF_6 (0.52 g, 3.2 mmol) was added to the yellow filtrate, and the volume was reduced to 15 mL. This was left to stand at 277 K for 6 h, during which time orange crystals formed (0.23 g, 37.7% yield). ^{1}H NMR (DMSO-d_6): δ 6.13 (b, 2H), 5.48 (d, 2H), 5.32 (d, 2H), 4.22 (b, 2H), 2.71 (m, 1H), 2.43 (m, 2H), 2.32 (m, 2H), 2.11 (s, 3H), 1.25 (d, 6H). Anal. Calcd for $C_{12}H_{22}ClF_6N_2PRu$: C, 30.29; H, 4.66; N, 5.88. Found: C, 30.05; H, 4.41; N, 5.98.

[(η^6-*p*-cymene)RuI($H_2NCH_2CH_2NH_2$−*N,N*)]PF_6 (6). The procedure followed that for compound **3** using [(η^6-*p*-cymene)-$RuI_2]_2$ (0.34 g, 0.35 mmol), ethylenediamine (0.06 g, 1 mmol), and NH_4PF_6 (0.52 g, 3.2 mmol). The volume was reduced to 15 mL and left to stand at 277 K overnight, during which time red crystals formed (0.24 g, 59.5% yield). Anal. Calcd for $C_{12}H_{22}IF_6N_2PRu$: C, 25.41; H, 3.91; N, 4.94. Found: C, 25.64; H, 3.72; N, 5.24.

[(η^6-*p*-cymene)$RuCl_2$(isonicotinamide)] (7). [(η^6-*p*-cymene)$RuCl_2]_2$ (0.129 g, 0.21 mmol) was stirred in benzene (50 mL), and isonicotinamide (0.052 g, 0.43 mmol) was added in one portion. The mixture was heated to reflux under argon for 4 h, during which time a mustard-colored precipitate formed. This was collected by filtration, washed with a little benzene, and recrystallized from methanol/ether to give red crystals (0.061 g, 33.8% yield). Anal. Calcd for $C_{16}H_{20}Cl_2N_2ORu$: C, 44.87; H, 4.71; N, 6.54. Found: C, 44.65; H, 4.54; N, 6.23.

[(η^6-$C_6H_5CO_2CH_3$)RuCl($H_2NCH_2CH_2NH_2$−*N,N*)]PF_6 (8). Ethylenediamine (0.09 g, 1.5 mmol) was added to a stirred suspension of [(η^6-$C_6H_5CO_2CH_3$)$RuCl_2]_2$ (0.355 g, 0.576 mmol) in methanol (200 mL). After 4 h the orange solution was filtered and the volume reduced to 20 mL. NH_4PF_6 (0.49 g, 2.3 mmol) was added, and the mixture was stirred for an additional minute. The sealed flask was left to stand overnight at 277 K. The resulting yellow microcrystalline solid was collected by filtration, washed with a little methanol followed by ether, and dried in vacuo (0.22 g, 40.0% yield). Anal. Calcd for $C_{10}H_{16}ClN_2O_2PF_6Ru$: C, 25.14; H, 3.38; N, 5.86. Found: C, 25.18; H, 3.12; N, 5.50.

[(η^6-$C_6H_5C_6H_5$)RuCl($H_2NCH_2CH_2NH_2$−*N,N*)]PF_6 (9). [(η^6-$C_6H_5C_6H_5$)$RuCl_2]_2$ (0.30 g, 0.46 mmol) was refluxed in H_2O (25 mL) for 1 h. At this time ethylenediamine (0.06 g, 1 mmol) was added to the refluxing suspension. The brown suspension immediately became dark-green. This was refluxed for another 30 min and filtered while hot. NH_4PF_6 (0.5 g, 3 mmol) was added to the yellowish filtrate, and the flask was briefly shaken. A yellow precipitate began to form almost immediately. The flask was sealed, allowed to cool to ambient temperature, and placed in an ice bath for 3 h. The precipitate was collected by filtration, washed with a little water followed by ethanol followed by ether, and dried in vacuo. It was recrystallized from methanol/ether (0.11 g, 23.9% yield). Anal. Calcd for $C_{14}H_{18}ClF_6N_2PRu$: C, 33.91; H, 3.66; N, 5.65. Found: C, 34.06; H, 3.37; N, 5.44.

[(η^6-$C_6H_5C_6H_5$)RuCl($H_2N(CH_2)_2NH(CH_2CH_3)$)]PF_6 (10). [(η^6-$C_6H_5C_6H_5$)$RuCl_2]_2$ (0.10 g, 0.158 mmol) was refluxed in water (10 mL) for 3 h and then cooled to 353 K. To this suspension was added *N*-ethylethylenediamine (37 mg, 0.42 mmol). The brown suspension immediately became dark-green. This was then slowly heated to reflux again for another 1.5 h and filtered while hot. NH_4PF_6 (0.2 g, 1.23 mmol) was added to the yellowish filtrate, and the flask was briefly shaken. A yellow precipitate began to form almost immediately. After the mixture was allowed to stand at 277 K overnight, the precipitate was collected by filtration, washed with a little methanol followed by diethyl ether, and dried in vacuo. This was recrystallized from methanol/ether (0.08 g, 48.3% yield). Anal. Calcd for $C_{16}H_{22}ClF_6N_2PRu$: C, 36.68; H, 4.23; N, 5.35. Found: C, 36.00; H, 4.37; N, 5.24.

Growth Inhibition Assays. Toxicity screens were carried out using the A2780 human adenocarcinoma cell line. The cells were grown as monolayers in RPMI 1640 medium with L-glutamine containing 5% fetal calf serum and a 1% antibiotic mixture. Cells were maintained under standard tissue culture conditions (37 °C, 5% CO_2), seeded in 24-well trays at a density of 1×10^4 cells per well, and allowed to grow for 72 h before addition of the Ru(II) complexes. Stock solutions of the ruthenium complexes were made up fresh in deionized water and sonicated to ensure complete dissolution. These stock solutions were diluted with RPMI medium to give final concentrations of 0.1, 1, 10, and 100 μM. All the compounds were evaluated at these concentrations in duplicate. Cisplatin was employed as a positive control because the cell line was known to be sensitive to this agent. The cells were exposed to the compounds for 24 h before the drug-containing medium was aspirated off. The cells were washed with phosphate-buffered saline (PBS), and fresh medium was added. The cells were counted on day 7 using a coulter counter.

DNA Binding. The concentrations of the oligonucleotides were determined using UV−vis spectroscopy: strand **I**, ϵ_{260} = 149.0 μM^{-1} cm^{-1}; strand **II**, ϵ_{260} = 137.2 μM^{-1} cm^{-1}. For the HPLC separation, reaction mixtures containing 100 μM **I** and the ruthenium complex were sealed in Eppendorf tubes and incubated at 310 K. To study the time dependence, aliquots were taken at various intervals over a total period of 2 days. For mass spectrometry, samples were diluted twice in HPLC grade CH_3CN prior to infusion. Concentrations of separated oligonucleotides used for enzyme digestion were typically ca. 25 μM, and 2 μL of VPD solution (diluted three times in H_2O) was added to 200 μL of the oligonucleotide solution. The mixtures were incubated at 310 K, and aliquots were extracted at various time intervals and diluted twice with CH_3CN prior to ESI-MS analysis.

For the DNA melting experiments, duplex **III** was incubated with either cisplatin or complex **5** for 4 days at ambient temperature in a 1:1 mole ratio (3 μM, 10 mM sodium phosphate buffer, pH 7.0, 50 mM $NaClO_4$).

Topoisomerase Assays. Inhibition of the catalytic activity of human DNA topoisomerase (Topo) I and II was evaluated by monitoring the enzyme-catalyzed relaxation of a supercoiled DNA substrate by 1% agarose gel electrophoresis as described previously in detail.[22] Stock solutions of compounds **5**, **6**, **8**, and **9** were made up fresh in phosphate-buffered saline (PBS) at a stock concentration of 500 μg/mL. Amsacrine (m-AMSA) was employed as a positive control for Topo II inhibition and NU/ICRF 506 as a positive control for Topo I inhibition.[22,28] Both these compounds were initially dissolved in DMSO, and cisplatin was also included for comparison. All compounds were evaluated at three different final concentrations, 1, 10, and 50 μM, and experimental procedures were repeated twice.

X-ray Crystallography. Standard data relating to the X-ray crystal structures of complexes **5**, **7**, and **9** have been deposited in the Cambridge Crystallographic Data Centre with CCDC reference numbers 170360, 170361, and 170362, respectively.

Acknowledgment. We thank the EPSRC, ICRF, EC COST Action D8 (Chemistry of Metals in Medicine), and CVCP (ORS Award for H.C.) for their support for this work, and Professor Martin Bennett (Australian National University), Dr. Abraha Habtemariam (Edinburgh), and members of COST Working Group D8/0018/98 for stimulating discussions.

Supporting Information Available: Figure S1 showing X-ray crystal structure of complex **5**, Figure S2 showing X-ray crystal structure of complex **7**, Figure S3 showing the HPLC study of the aquation of complex **5**, Figure S4 showing LC−ESI-MS of complex **5** in water, Figure S5 showing VPD digestion ladder for peak e in Figure 2. This material is available free of charge via the Internet at http://pubs.acs.org.

References

(1) Clarke, M. J.; Zhu, F.; Frasca, D. R. Non-platinum chemotherapeutic metallopharmaceuticals. *Chem. Rev.* **1999**, *99*, 2511−2534.

(2) Clarke, M. J. Oncological implications of the chemistry of ruthenium. *Met. Ions Biol. Syst.* **1980**, *11*, 231−283.

(3) Keppler, B. K.; Henn, M.; Juhl, U. M.; Berger, M. R.; Niebl, R.; Wagner, F. E. New ruthenium complexes for the treatment of cancer. *Prog. Clin. Biochem. Med.* **1989**, *10*, 41−69.

(4) Novakova, O.; Kasparkova, J.; Vrana, O.; Van Vliet, P. M.; Reedijk, J.; Brabec, V. Correlation between cytotoxicity and DNA binding of polypyridyl ruthenium complexes. *Biochemistry* **1995**, *34*, 12369−12378.

(5) Vilaplana, R. A.; González-Vílchez, F.; Gutierrez-Puebla, E.; Ruiz-Valero, C. The first isolated antineoplastic Ru(IV) complex: synthesis and structure of $[Cl_2$(1,2-cyclohexanediaminotetraacetate)Ru]·$2H_2O$. *Inorg. Chim. Acta* **1994**, *224*, 15−18.

(6) Sava, G.; Gagliardi, R.; Bergamo, A.; Alessio, E.; Mestroni, G. Treatment of metastases of solid mouse tumours by NAMI-A: comparison with cisplatin, cyclophosphamide and dacarbazine. *Anticancer Res.* **1999**, *19*, 969−972.

(7) Smith, C. A.; SunderlandSmith, A. J.; Keppler, B. K.; Kratz, F.; Baker, E. N. Binding of ruthenium(III) antitumor drugs to human lactoferrin probed by high resolution X-ray crystallographic structure analyses. *J. Biol. Inorg. Chem.* **1996**, *1*, 424−431.

(8) Messori, L.; Kratz, F.; Alessio, E. The interaction of the antitumor complexes Na[*trans*-$RuCl_4$(DMSO)(Im)] and Na[*trans*-$RuCl_4$(DMSO)(Ind)] with apotransferrin: a spectroscopic study. *Met.-Based Drugs* **1996**, *3*, 1−9.

(9) Frasca, D.; Ciampa, J.; Emerson, J.; Umans, R. S.; Clarke, M. J. Effects of hypoxia and transferrin on toxicity and DNA binding of ruthenium antitumor agents in HeLa cells. *Met.-Based Drugs* **1996**, *3*, 197−209.

(10) Kramer, R.; Maurus, M.; Polborn, K.; Sunkel, K.; Robl, C.; Beck, W. Organometallic half-sandwich complexes promote the formation of linear oligopeptides from amino acid esters. *Chem.—Eur. J.* **1996**, *2*, 1518−1526.

(11) Sheldrick, W. S.; Heeb, S. Synthesis and structural characterization of η^6-arene-ruthenium(II) complexes of α-amino acids with coordinating side chains. *J. Organomet. Chem.* **1989**, *377*, 357−366.

(12) Plitzko, K. D.; Wehrle, G.; Gollas, B.; Rapko, B.; Dannheim, J.; Boekelheide, V. Bis(η^6-hexamethylbenzene)(η^6,η^6-polycyclic aromatic)diruthenium(II,II) complexes and their two-electron reduction to cyclohexadienyl anion complexes. *J. Am. Chem. Soc.* **1990**, *112*, 6556−6564.

(13) Porter, L. C.; Bodige, S.; Selnau, H. E. Preparation of new bis(arene)ruthenium(II) complexes. X-ray crystal structures of [(η^6-biphenyl)$_2$Ru][BF_4]$_2$ and the syn and anti isomers of [(η^6-fluorene)$_2$Ru][BF_4]$_2$. *Organometallics* **1995**, *14*, 4222−4227.

(14) Charbonneau, G.-P.; Delugeard, Y. Structural transition in polyphenyls. III. Crystal structure of biphenyl at 110 K. *Acta Crystallogr.* **1976**, *B32*, 1420−1423.

(15) Hung, Y.; Kung, W.-J.; Taube, H. Aquo chemistry of monoarene complexes of osmium(II) and ruthenium(II). *Inorg. Chem.* **1981**, *20*, 457−463.

(16) Korn, S.; Sheldrick, W. S. pH-Dependent competition between κ^2N^7,*O(P)* macrochelation and μ-N^1,N^7 oligomer formation for (η^6-arene)Ru^{II} complexes of adenosine and guanosine 5′-mono-, -di- and -tri-phosphates. *J. Chem. Soc., Dalton Trans.* **1997**, 2191−2199.

(17) Anagnostopoulou, A.; Moldrheim, E.; Katsaros, N.; Sletten, E. Interaction of *cis*- and *trans*-$RuCl_2(DMSO)_4$ with the nucleotides GpA, d(GpA), ApG, d(ApG) and d(CCTGGTCC): high-field NMR characterization of the reaction products. *J. Biol. Inorg. Chem.* **1999**, *4*, 199−208.

(18) Hartmann, M.; Einhäuser, T. J.; Keppler, B. K. Two antitumour ruthenium(III) complexes showing selectivity in their binding towards poly(dG) poly(dC) and poly(dA) poly(dT). *Chem. Commun.* **1996**, 1741−1742.

(19) Andersen, B.; Margiotta, N.; Coluccia, M.; Natile, G.; Sletten, E. Antitumor *trans* platinum DNA adducts: NMR and HPLC study of the interaction between a *trans*-Pt iminoether complex and the deoxy decamer d(CCTCGCTCTC)·d(GAGAGCGAGG). *Met.-Based Drugs* **2000**, *7*, 23−32.

(20) Wang, J. C. DNA topoisomerases. *Annu. Rev. Biochem.* **1985**, *54*, 665−697.

(21) Wang, J. C. DNA topoisomerases. *Annu. Rev. Biochem.* **1996**, *65*, 635−692.

(22) Meikle, I.; Cummings, J.; MacPherson, J.; Hadfield, J. A.; Smyth, J. F. Biochemistry of topoisomerase-I and topoisomerase-II inhibition by anthracenyl-amino acid conjugates. *Biochem. Pharmacol.* **1995**, *49*, 1747−1757.

(23) Gopal, Y. N. V.; Jayaraju, D.; Kondapi, A. K. Inhibition of topoisomerase II catalytic activity by two ruthenium compounds: a ligand-dependent mode of action. *Biochemistry* **1999**, *38*, 4382−4388.

(24) Bennett, M. A.; Smith, A. K. Arene ruthenium(II) complexes formed by dehydrogenation of cyclohexadienes with ruthenium(III) trichloride. *J. Chem. Soc., Dalton Trans.* **1974**, 233−241.

(25) Zelonka, R. A.; Baird, M. C. Benzene complexes of ruthenium(II). *Can. J. Chem.* **1972**, *50*, 3063−3072.

(26) McCormick, F. B.; Cox, D. D.; Gleason, W. B. Synthesis, structure, and disproportionation of labile (η^6-C_6H_6)Ru(CH_3CN)$_2Cl^+$ salts. *Organometallics* **1993**, *12*, 610−612.

(27) Solorzano, C.; Davis, M. A. Preparation of arene ruthenium(II) complexes with activated ligands for protein labeling. *Inorg. Chim. Acta* **1985**, *97*, 135−141.

(28) Cummings, J.; MacPherson, J. S.; Meikle, I.; Smyth, J. F. Development of anthracenyl-amino acid conjugates as topoisomerase I and II inhibitors that circumvent drug resistance. *Biochem. Pharmacol.* **1996**, *52*, 979−990.

JM010051M